

Inclusive π^0 production in π^-p and π^+p interactions at 18.5 GeV/c[†]

N. N. Biswas, E. D. Fokitis, J. M. Bishop, N. M. Cason, V. P. Kenney, and W. D. Shephard

Department of Physics, University of Notre Dame, Notre Dame, Indiana 46556

(Received 26 June 1974)

We have studied π^0 production in 18.5-GeV/c π^-p and π^+p interactions by using the photons from π^0 decay which convert to electron pairs in hydrogen. The inclusive π^0 cross sections for different charged multiplicities have been determined. The dependence of the invariant cross section on the Feynman scaling variable x is presented. The π^0 production process is compared with π^- and π^+ production for each reaction. We observe that the π^0 spectrum is similar to the π^+ spectrum in π^-p interactions and to the π^- spectrum in π^+p interactions.

I. INTRODUCTION

In this paper we study the inclusive π^0 production processes

$$\pi^-p \rightarrow \pi^0 + \text{anything}, \quad (1a)$$

and

$$\pi^+p \rightarrow \pi^0 + \text{anything} \quad (1b)$$

at an incident momentum of 18.5 GeV/c. At the same energy, we have previously studied^{1, 2} the charged pion inclusive reactions,

$$\pi^-p \rightarrow \pi^\pm + \text{anything}, \quad (2a)$$

and

$$\pi^+p \rightarrow \pi^\pm + \text{anything}. \quad (2b)$$

In this study we compare the inclusive spectra of the three isospin states of pions with one another.

Experimentally we observe electron pairs from photons, presumably arising from π^0 decay, which convert in a hydrogen bubble chamber. Results on the inclusive production of neutral particles K_1^0 , Λ^0 , and $\bar{\Lambda}^0$ have been reported elsewhere.³ We will be concerned here with the process

$$\pi^\pm p \rightarrow \gamma + \text{anything} \quad (3)$$

as well as reactions (1a) and (1b).

In Sec. II we present the experimental procedure. In Sec. III we determine the π^0 inclusive cross section from γ inclusive cross sections. We present γ inclusive spectra in Sec. IV and discuss the relation of the π^0 spectrum with the γ spectrum. In Sec. V we report the π^0 spectrum as determined directly from events in which both the γ 's from π^0 decays are observed. We present in Sec. VI the over-all average transverse momenta of photons and of pions of all charges. Finally, in Sec. VII we summarize the results and present our conclusions.

II. EXPERIMENTAL PROCEDURE

The film used in this experiment was obtained from Brookhaven National Laboratory. The 80-in. hydrogen bubble chamber was exposed to an un-separated 18.5-GeV/c π^- beam and a separated 18.5-GeV/c π^+ beam from the Alternating Gradient Synchrotron. A total of 152 000 pictures with π^- beam and a total of 170 000 pictures with π^+ beam were taken. The data presented here are obtained from about half of each of these exposures. We have scanned the pictures for events associated with secondary V decays. During scanning, all events associated with possible electron pairs were recorded. A neutral V decay was rejected only when the V could be obviously identified as a strange particle (e.g., large opening angle and/or the presence of a heavily ionizing positively charged track). In the case of events with multiple V decays, if any of the V 's satisfied the criteria for an electron pair, the event was recorded. Further, if an electron pair was seen in a frame having multiple primary interactions, each of these events was recorded as being possibly associated with the pair unless the γ could obviously not have come from the primary vertex. Thus, at the scanning stage, a significant fraction of the scanned events (~15%) involves V 's which are not truly associated with the primary vertex. Such events were eliminated by geometric reconstruction.

We have measured 7495 events in π^-p interactions and 10 083 events in π^+p interactions to obtain a sample of genuine γ -associated events. These measured events were processed using the geometrical reconstruction program TVGP and the kinematic fitting program SQUAW. The events in which V fitted an electron pair and pointed back to a primary vertex were accepted. About 1% of the V 's fit both the electron pair and K^0 hypotheses. These events are assumed to be electron pairs. The events which failed in TVGP as well as the events which failed in SQUAW as associated- V events were measured for a second time. These

remeasured events were again processed through TVGP and SQUAW, and the associated events were accepted; the failed events were finally rejected. Using events from these two measurements, we obtained a final sample of 5750 events in π^-p interactions and 7314 in π^+p interactions with at least one associated V . The present study is based on these samples.

III. INCLUSIVE γ AND π^0 CROSS SECTIONS

To obtain absolute cross sections, we need to determine the cross section per event and various correction factors. In this study we have used the same sample of π^-p and π^+p pictures used in a previous study¹ of π^- inclusive production. (A slight renormalization was necessary for various reasons; e.g., some pictures could not be used due to the deterioration of the film.) We have thus used the previously determined cross section per event, suitably renormalized, and have made the following corrections:

(a) *Scanning efficiency.* About one-third of the film used in the study was rescanned and a comparison of the two scans was made. We find the over-all single-scan efficiency for associated electron pairs is 72.4% in the π^-p sample and 74.3% in the π^+p sample. However, the scanning efficiency was found to be dependent on prong number. In particular the efficiencies for the 0-prong and 2-prong events in the π^-p case and for the 2-prong events in the π^+p case are significantly lower than the over-all efficiencies. Thus it was necessary to introduce correction factors dependent on prong number for scanning efficiencies. The single-scan efficiencies as a function of prong number are listed in Table I.

(b) *Measuring and reconstruction efficiency.* The combined TVGP and SQUAW efficiencies for genuine V -associated events determine the measuring and reconstruction efficiency. In calculating this, we have assumed that the TVGP geometrical-reconstruction efficiency is the same for V -associated and nonassociated events, since no association of primary and secondary vertices is demanded in this program. The TVGP efficiency is thus obtained by noting the number of events measured and the number of events successfully reconstructed by the program. In SQUAW the association of a V with primary vertex is necessary. We assume that the efficiency for a non-associated V event is zero⁴ and then determine the efficiency for associated events. Thus the total number of events failing in TVGP and SQUAW is assumed to contain all nonassociated events as well as associated events due to SQUAW inefficiency. Events which failed initially were remea-

TABLE I. Single-scan efficiencies.

Prong	π^-p reaction	π^+p reaction
0	0.555 ± 0.103	...
2	0.676 ± 0.018	0.690 ± 0.016
4	0.734 ± 0.013	0.753 ± 0.011
6	0.752 ± 0.016	0.754 ± 0.013
≥ 8	0.742 ± 0.026	0.779 ± 0.020

sured and reprocessed. By noting the number of events at each stage of processing, we can determine the TVGP efficiencies for each of the two measurements. Assuming that the SQUAW efficiencies for associated events are the same for both measurements (and zero for nonassociated events), we can determine the over-all SQUAW efficiency for the γ -associated events in the sample. We find that the combined TVGP and SQUAW efficiency is $\sim 91\%$ in both reactions. All cross sections have been corrected for this loss. Using

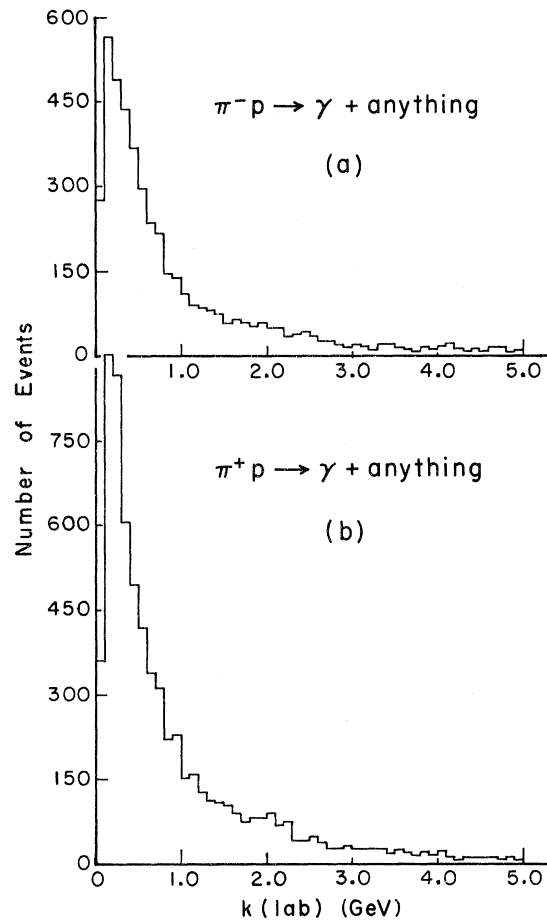


FIG. 1. Laboratory energy distribution of photons in (a) 18.5-GeV/c π^-p interactions and (b) 18.5-GeV/c π^+p interactions.

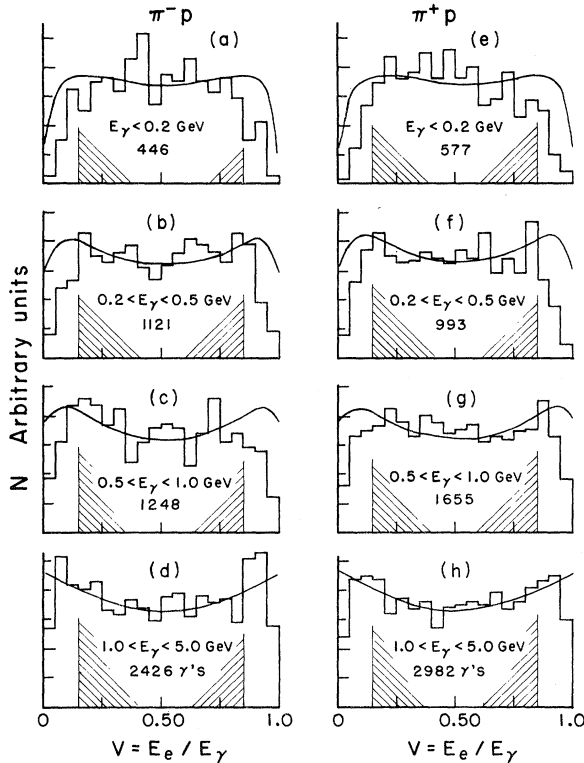


FIG. 2. Distributions of $V = E_e/E_\gamma$, the fractional energy of the conversion electron from a γ of energy E_γ for various ranges of E_γ . (a)–(d) correspond to π^-p interactions and (e)–(h) to π^+p interactions. The curves represent theoretical calculations for expected distributions. In all the distributions the data and curves are normalized to the same area in the region $0.15 < V \leq 0.85$.

this efficiency we can determine the actual number of events with associated electron pairs as well as the number of nonassociated events. We find that the sample of processed events consists of $\sim 16\%$ nonassociated events in the π^-p case and of $\sim 20\%$ nonassociated events in the π^+p case. An independent check as to the consistency of these numbers can be made using scanning information. We find that in $\sim 12\%$ of the cases, a single γ is assigned at the scanning stage to more than one event occurring in a single frame; this is expected to be the lower limit for the fraction of nonassociated events and is consistent with the computed numbers.

(c) *Photon conversion probability.* The electron pair conversion probability for each γ has been calculated using quantum electrodynamics⁵ as a function of γ energy and of the potential length available. The calculated conversion cross section has been checked with the experimental data of Knasel.⁶ In our experiment the average over-all weight factor for an event (the inverse of the probability for conversion) is about 22.5.

TABLE II. Correction factors for electron pair loss.

E_γ (GeV)	Correction factor for π^-p reaction	Correction factor for π^+p reaction
< 0.2	1.154	1.175
$0.2-0.5$	1.164	1.181
$0.5-1.0$	1.135	1.114
$1.0-5.0$	1.006	1.038

(d) *Loss of electron pairs from γ conversion.* This loss has been determined from the comparison of electron spectra with the expected theoretical distributions. The distributions of laboratory energy of γ 's, E_γ , are shown in Figs. 1(a) and 1(b) for the π^-p and the π^+p reactions, respectively. For different intervals of E_γ , we have plotted in Fig. 2 the distributions of $V = E_e/E_\gamma$ (where E_e is the energy of the electron). Figures 2(a)–2(d) correspond to π^-p data and Figs. 2(e)–2(h) to π^+p data. The curves shown are taken from Rossi,⁷ and have been normalized to the data in the region $0.15 < V < 0.85$. Loss of events occurs as the electron or positron energy tends to zero, in particular for low γ energy. Comparison of theoretical curves with the data of Fig. 2 yields the correction factors shown in Table II.

The single- γ inclusive cross sections obtained after these corrections and the average number of γ 's per inelastic event⁸ are shown in Table III, as a function of n , the number of charged particles. The over-all average number of γ 's per inelastic event is 3.61 ± 0.16 for π^-p reactions and 3.44 ± 0.23 for π^+p reactions. Assuming that π^0 mesons are the sole source of γ 's, the inclusive π^0 cross sections and average π^0 multiplicities as a function of n are equal to half the corresponding γ cross sections and multiplicities. The over-all inclusive π^0 cross sections and average π^0 multiplicities are $\sigma(\pi^0) = 38.20 \pm 1.50$ mb, $\langle n_{\pi^0} \rangle = 1.80 \pm 0.08$ for π^-p interactions and $\sigma(\pi^0) = 33.85 \pm 1.90$ mb, $\langle n_{\pi^0} \rangle = 1.72 \pm 0.12$ for π^+p interactions.

The dependence of $\langle n_\gamma \rangle$ on prong number n is shown in Figs. 3(a) and 3(b) for π^-p and π^+p reactions. We observe that, for both reactions, $\langle n_\gamma \rangle$ does not show strong dependence on n . The data on π^0 production are, at present, rather meager. This is more so for π^\pm and K^\pm reactions than for pp reactions. The available π^0 data⁹⁻¹² for pp , πp , and Kp interactions in the energy range of this investigation show an n dependence of $\langle n_\gamma \rangle$ similar to that observed here [Figs. 3(a) and 3(b)]. At higher energies, π^0 data are primarily available for pp interactions and $\langle n_\gamma \rangle$ is found⁹ to increase with increasing n . In Fig. 3(c) we show available data⁹⁻¹² for the over-all π^0 multiplicity as a function of incident beam momentum. The

TABLE III. Inclusive γ cross sections for 18.5-GeV/c π^-p and π^+p reactions.

n	π^-p interactions			π^+p interactions		
	Observed γ 's	Inclusive cross section (mb)	$\langle n_\gamma \rangle$	Observed γ 's	Inclusive cross section (mb)	$\langle n_\gamma \rangle$
0	77	1.23 ± 0.46	3.50 ± 1.54
2	1258	16.51 ± 1.21	3.66 ± 0.41	1362	13.72 ± 0.89	4.38 ± 0.98
4	2252	30.19 ± 2.05	3.29 ± 0.24	2729	26.12 ± 1.55	2.89 ± 0.20
6	1549	20.52 ± 1.45	3.90 ± 0.30	2133	20.52 ± 1.25	3.70 ± 0.26
8	494	6.89 ± 0.59	4.36 ± 0.40	646	6.29 ± 0.45	3.83 ± 0.31
10	76	0.94 ± 0.13	3.51 ± 0.51	104	0.96 ± 0.11	3.37 ± 0.41
12	8	0.12 ± 0.05	4.17 ± 1.69	10	0.08 ± 0.02	2.42 ± 0.81
14	1	0.01 ± 0.01	...
Total	5714	76.40 ± 2.90		6985	67.70 ± 3.80	

data are qualitatively consistent with a logarithmic increase of $\langle n_{\pi^0} \rangle$ with laboratory momentum.

It is of interest to compare the inclusive cross sections for inclusive production of π^- , π^+ , and π^0 mesons from the same reaction. In Table IV we show these cross sections for 18.5-GeV/c π^-p and π^+p interactions. The errors shown in Table IV are statistical only. The quantity $\frac{1}{2}[\sigma(\pi^-) + \sigma(\pi^+)]$ is also shown in the table. In π^-p interactions $\sigma(\pi^0)$ is inconsistent with the value of $\sigma(\pi^-)$ and is

consistent with the value of $\sigma(\pi^+)$. For π^+p interactions $\sigma(\pi^0)$ is inconsistent with the value of $\sigma(\pi^+)$, and seems only slightly higher than the value of $\sigma(\pi^-)$.

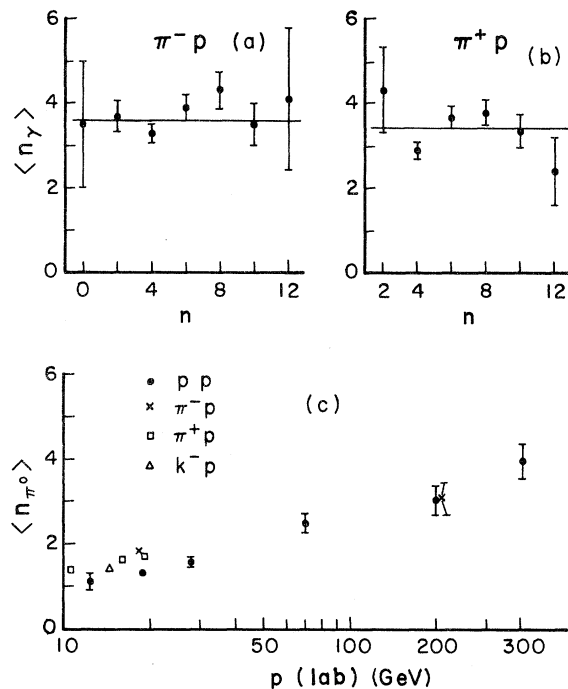


FIG. 3. Average number of γ 's per inelastic event as a function of charged prong number n for (a) 18.5-GeV/c π^-p interactions, and (b) 18.5-GeV/c π^+p interactions. (c) The average number of π^0 's per inelastic event is shown as a function of incident particle momentum for various reactions.

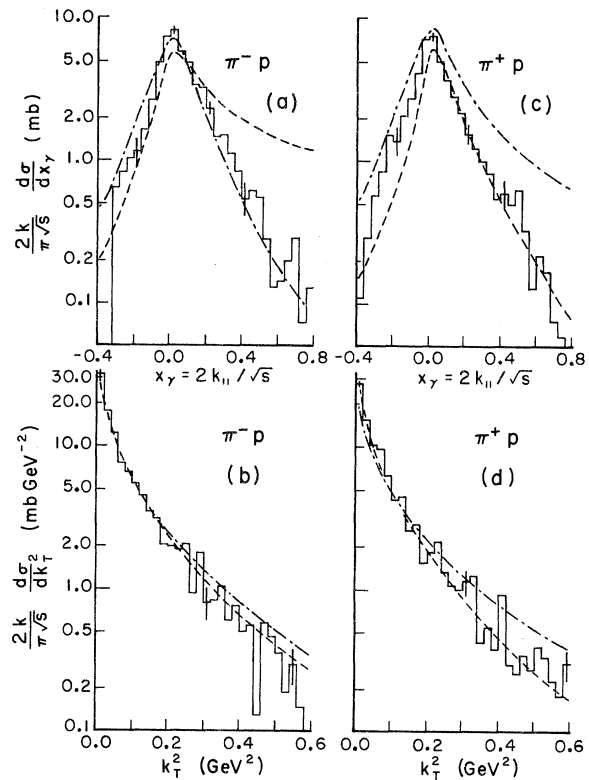


FIG. 4. Invariant differential cross section for γ production as a function of (a) x_γ and (b) k_T^2 in 18.5-GeV/c π^-p interactions and (c) x_γ and (d) k_T^2 in 18.5 GeV/c π^+p interactions. The histograms represent the data. The dashed curves represent Monte Carlo calculations using inclusive π^- production distributions to simulate π^0 production; the dot-dashed curves represent calculations using inclusive π^+ distributions to simulate π^0 production.

TABLE IV. Inelastic pion inclusive cross sections at 18.5 GeV/c.^a

Reaction	$\sigma(\pi^-)$ (mb)	$\sigma(\pi^+)$ (mb)	$\sigma(\pi^0)$ (mb)	$\frac{1}{2}[\sigma(\pi^-) + \sigma(\pi^+)]$ (mb)
π^-p	46.47 ± 1.66	40.50 ± 1.60	38.20 ± 1.50	43.48 ± 1.21
π^+p	26.37 ± 1.33	57.66 ± 3.52	33.85 ± 1.90	42.01 ± 1.88

^a From Refs. 1 and 2.IV. INCLUSIVE γ SPECTRUM

We present the inclusive γ spectra in Fig. 4 in terms of the variables $x_\gamma = 2k_{\parallel}/\sqrt{s}$ and k_T^2 , where k_{\parallel} and k_T are the longitudinal and transverse components of photon momentum in the over-all center-of-mass system. Figures 4(a) and 4(b) show the invariant differential cross sections as a function of x_γ and k_T^2 respectively for π^-p interactions. Figures 4(c) and 4(d) show similar distributions for π^+p interactions.

Two curves are shown in each of Figs. 4. These curves correspond to γ spectra derived with the assumptions that the π^0 spectrum is the same as (a) the π^- spectrum (dashed curve) and (b) the π^+ spectrum (dot-dashed curve). To generate these curves, we have used the experimental data^{1,2} for π^- and π^+ inclusive production as observed in these reactions. Assuming the momentum of a π^0 to be that of a π^- or a π^+ , we calculate the γ spectrum by a Monte Carlo method. Two random numbers are generated to fix the decay angles (with respect to the π^0 momentum vector) of the process $\pi^0 \rightarrow 2\gamma$ in the π^0 rest frame and then the energy-momentum vectors of both γ 's are calculated. In this way we have generated four samples of γ 's utilizing π^- (π^+) spectra for π^-p and π^+p interactions to simulate the π^0 spectra. Each sample consists of 30 000 γ 's corresponding to 15 000 charged-pion momentum vectors. Using these events we have plotted histograms of inclusive γ cross sections. The generated histograms do not show fluctuations and hence smooth curves have been drawn by hand through the distributions. The resulting smooth curves are shown in Fig. 4 and they represent the inclusive γ cross sections expected if the π^0 production were the same as the production of π^- (π^+) in terms of cross section as well as momentum distribution.

Comparing the experimental x_γ distributions with the curves, we find that the observed π^0 spectrum is rather similar, particularly in the forward direction, to the spectrum generated from produced π^+ in π^-p reactions and to the spectrum generated from produced π^- in π^+p interactions [Figs. 4(a) and 4(c)]. The k_T^2 distributions for produced γ 's [Figs. 4(b) and 4(d)] are insensitive

to the variations of the π^0 momentum distribution considered here.

V. INCLUSIVE π^0 SPECTRA

In the above discussion a comparative study of π^0 , π^- , and π^+ spectra was made using γ spectra. We now attempt a direct comparison of the π^0 spectrum with π^- and π^+ spectra.

A. Inclusive π^0 spectra derived from γ spectra

The invariant π^0 differential cross section can be derived from the measured γ spectrum over a limited kinematic region. The relation between γ and π^0 spectra has been discussed by many

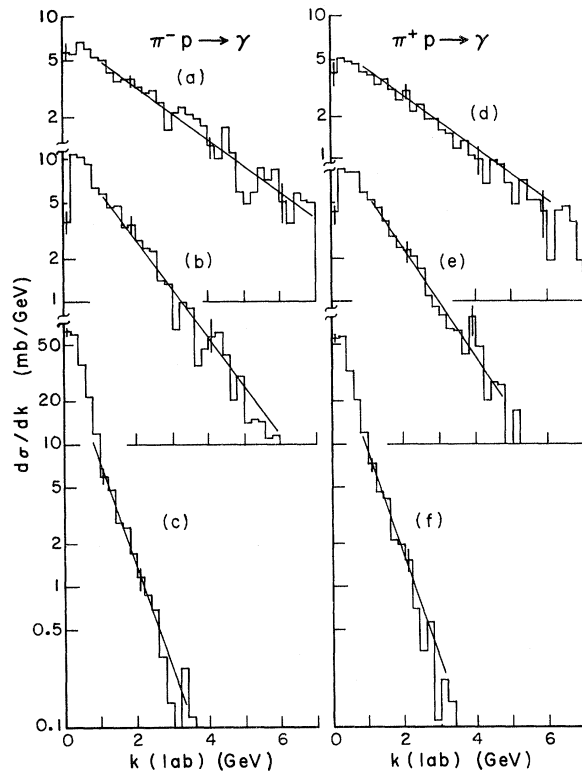


FIG. 5. Distributions of $d\sigma/dk$ as a function of laboratory photon momentum k in 18.5-GeV/c π^-p interactions, (a)–(c), and π^+p interactions, (d)–(f). Distributions are shown for three ranges of photon production angles: (a), (d): $0.995 < \cos\theta < 1.0$; (b), (e): $0.980 < \cos\theta < 0.995$; and (c), (f): $0.92 < \cos\theta < 0.98$. The curves represent fits to the data described in the text.

TABLE V. Parameters of γ and π^0 spectra in the laboratory frame.

cos θ interval	π^-p reaction			π^+p reaction		
	A (GeV $^{-1}$)	B (GeV $^{-1}$)	C (mb GeV $^{-2}$)	A (mb GeV $^{-1}$)	B (GeV $^{-1}$)	C (mb GeV $^{-2}$)
0.995–1.0	7.41 \pm 1.04	0.41 \pm 0.07	1.53 \pm 0.34	5.87 \pm 0.75	0.39 \pm 0.06	1.14 \pm 0.25
0.980–0.995	13.86 \pm 2.01	0.78 \pm 0.08	5.40 \pm 0.95	13.63 \pm 1.80	0.89 \pm 0.07	6.05 \pm 0.93
0.920–0.980	38.97 \pm 8.13	1.68 \pm 0.13	32.66 \pm 7.27	50.66 \pm 8.96	1.79 \pm 0.11	45.24 \pm 8.47
all	39.87 \pm 4.26	0.82 \pm 0.05	16.40 \pm 2.07	41.76 \pm 3.95	0.91 \pm 0.05	19.10 \pm 2.09

authors.^{13, 14} From kinematical considerations, Sternheimer¹³ has shown that the invariant π^0 cross section is simply related to the γ cross section for large π^0 or γ momenta. We consider here the laboratory frame and denote p and k as the magnitudes of momenta of the π^0 and γ , respectively. The choice of the laboratory frame is motivated by the fact that a relatively large fraction of the π^0 or γ spectra lies in the high-momentum region, and that the observed angle of the γ relative to the

beam direction is essentially the same as the angle of production of the π^0 . The invariant differential π^0 cross section given by $f(p, \cos\theta) \equiv E d^2\sigma/p^2 dp d\cos\theta$ is related to the γ cross section $d^2\sigma/dk d\cos\theta$ by the relation

$$f(p, \cos\theta) = -\frac{1}{2} \frac{d}{dk} (d^2\sigma/dk d\cos\theta). \quad (4)$$

Using these expressions we now derive the π^0 cross section, $f(p, \cos\theta)$, from the γ spectrum using data for $k \gg m_\pi$ (the pion mass).

We plot in Fig. 5 the γ cross section $d\sigma/dk$ for three different intervals of $\cos\theta$ in each of the re-

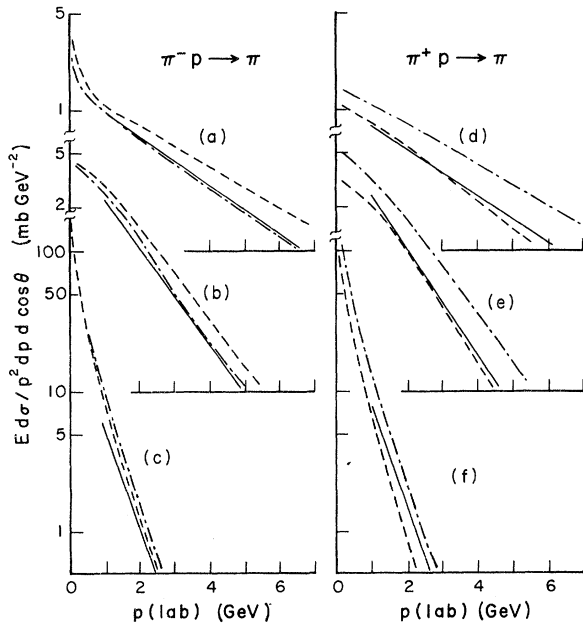


FIG. 6. The invariant cross section for π^- (dashed curves), π^+ (dot-dashed curves), and π^0 (solid curves) production as a function of laboratory momentum p . The data are shown for several ranges of $\cos\theta$, where θ is the laboratory production angle: $0.995 < \cos\theta < 1.0$ [(a) and (d)], $0.980 < \cos\theta < 0.995$ [(b) and (e)], and $0.92 < \cos\theta < 0.98$ [(c) and (f)]. (a)–(c) are for π^-p interactions, (d)–(f) are for π^+p interactions. The π^- and π^+ production data are direct measurements from previous experiments, and the π^0 production data are derived from the γ spectra using the Sternheimer approximation. Uncertainties for the solid-curve data are typically 0.16, 0.30, 0.44, 0.15, 0.28, 0.42 mb GeV $^{-2}$ at $p^{(\text{lab})} = 2\text{GeV}/c$ for (a), (b), (c), (d), (e), and (f), respectively.

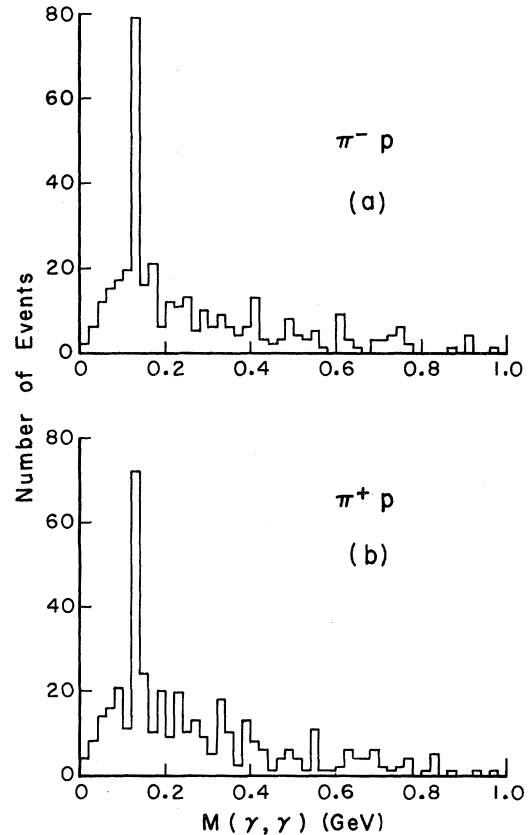


FIG. 7. Distributions of effective mass $M(\gamma\gamma)$ for (a) 18.5-GeV/ c π^-p events and (b) 18.5-GeV/ c π^+p events in which two γ 's are observed.

actions. The $\cos\theta$ intervals chosen are $0.995 < \cos\theta < 1.00$, $0.980 < \cos\theta < 0.995$, and $0.92 < \cos\theta < 0.98$. Figures 5(a)–5(c) correspond to π^-p interactions and Figs. 5(d)–5(f) to π^+p interactions. It is found that for $k > 1.0$ GeV, a region where the Sternheimer approximation should be applicable, the distribution of $d\sigma/dk$ follows a simple exponential. We have fitted these distributions with the form

$$d\sigma/dk = A \exp(-Bk) . \quad (5)$$

Using this simple expression, the π^0 spectrum is given by

$$f(p, \cos\theta) = (AB/2) \exp(-Bp) = C \exp(-Bp) . \quad (6)$$

The fitted parameters A and B found by fitting Eq. (5) to the data in the region $1.0 < k < 4.0$ GeV and the computed normalization factor C are shown in Table V.

Using the values of B and C from Table V we can compute the π^0 differential cross section and compare this with the observed π^- and π^+ inclusive spectra. In Fig. 6 we show the π^- , π^+ , and π^0 inclusive spectra for three different $\cos\theta$ intervals. The π^- and π^+ spectra shown here are the results of hand drawn curves through the actual experimental data and the π^0 spectra are derived from expression (6) in the region $p > 1$ GeV/c. We stress that in Fig. 6, we are dealing with the absolute π^0 inclusive cross section as well as its shape to the accuracy of the validity of the Sternheimer approximation and the adequacy of the parametrization of expression (5). We observe from Figs. 6(a) and 6(b) that for π^-p interactions, the π^0 spectra are in excellent agreement with the π^+ spectra. Similarly, in Figs. 6(d) and 6(e), the π^0 spectra in π^+p interactions are in excellent agreement with the π^- spectra. Figures 6(c) and 6(f) correspond to large-angle inclusive cross sections and hence the most γ or π^0 momenta are relatively low. No definite conclusion can be drawn as to the comparison of the π^0 spectra with π^- and π^+ spectra in this kinematic region.

B. Inclusive π^0 spectra from $\pi^0 \rightarrow 2\gamma$ events

A direct measurement of the π^0 spectrum can be made by using events where both of the γ 's from π^0 decay are observed. In Figs. 7(a) and 7(b) we show the observed effective-mass distributions of 2γ for π^-p and π^+p reactions. We observe a distinct signal for the π^0 meson at a mass of 0.135 GeV. We find that in π^-p interactions, 99 events out of 360 two- γ events have $0.12 < M(\gamma\gamma) < 0.15$ GeV (π^0 mass region). In π^+p reactions, 118 events out of 393 two- γ events are in the π^0 mass region. Using these events we can directly determine the

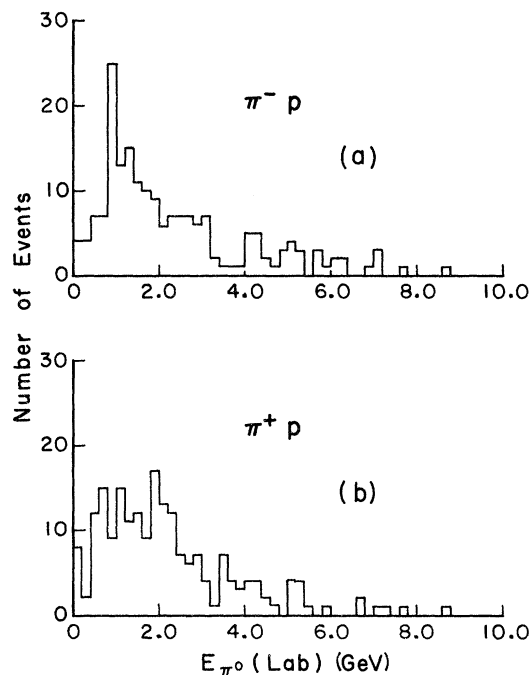


FIG. 8. Laboratory energy distributions of π^0 's obtained from 2γ events in (a) π^-p interactions and (b) π^+p interactions.

π^0 energy distribution as shown in Fig. 8.

These events are rather useful for the study of inclusive π^0 -meson production in a direct manner. Although one can, in principle, determine the inclusive π^0 cross section using the combined conversion probability of the two γ 's from π^0 decay, such a determination is dependent on the determination of π^0 signal in the $M(\gamma\gamma)$ distribution and also involves low statistics and large weight factors. Therefore in determining the π^0 differential cross sections from 2γ events we have used the narrow $M(\gamma\gamma)$ mass region to insure a pure sample of π^0 's and have normalized the resulting distributions to the inclusive π^0 cross sections of Table IV.

We plot in Figs. 9(a) and 9(b) the π^0 invariant cross sections as a function of x for the π^-p and π^+p interactions, respectively. We have checked that the shape of the x distribution does not significantly depend on the choice of the mass interval for $M(\gamma\gamma)$ within reasonable limits. In Fig. 9 we also show the experimental x distributions of π^- and π^+ by smooth curves for direct comparison. The uncertainties in the data points for the π^0 spectra are large due to the small number of events. Nevertheless, we may conclude that the π^0 distributions deviate markedly from the π^- distribution in π^-p interactions and from the π^+ distribution in π^+p interactions.

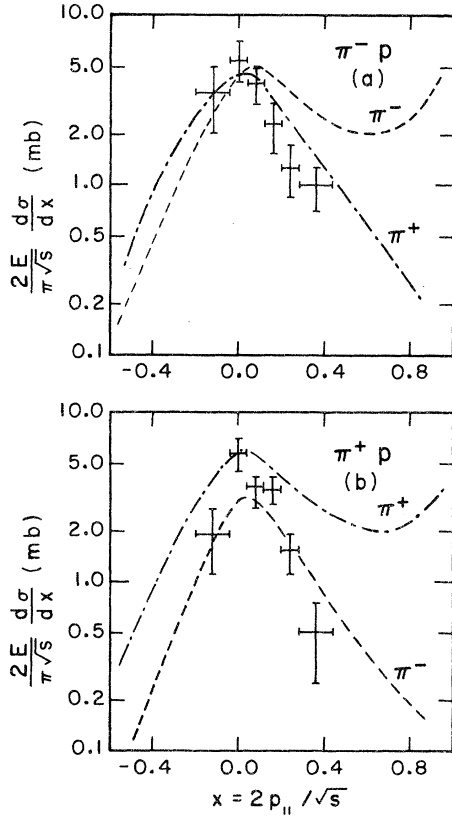


FIG. 9. Invariant differential cross sections for π^0 (experimental points), π^- (dashed curves), and π^+ (dot-dashed curves) production as a function of x for (a) 18.5-GeV/c π^-p interactions and (b) 18.5-GeV/c π^+p interactions. The π^0 production data are determined from $\pi^0 \rightarrow 2\gamma$ events where both γ 's are observed. The π^- and π^+ data are direct measurements from previous experiments.

VI. AVERAGE TRANSVERSE MOMENTA OF PIONS AND PHOTONS

In Table VI we show the over-all average transverse momenta of pions and photons for π^-p and π^+p reactions.¹⁵ The quoted errors are statistical only. The values for π^0 mesons have been derived from the $\pi^0 \rightarrow 2\gamma$ events (see Sec. V); the values for γ 's have been determined using all γ 's. The

values of $\langle p_T^2 \rangle$ for π^0 's can also be calculated from the values of $\langle k_T^2 \rangle$ for γ 's from the relation derived by Kopylov¹⁶:

$$\langle p_T^2 \rangle_{\pi^0} = 3\langle k_T^2 \rangle - m^2(\pi^0)/2. \quad (7)$$

We find these values to be $\langle p_T^2 \rangle_{\pi^0} = 0.147 \pm 0.003$ GeV²/c² in π^-p interactions and $\langle p_T^2 \rangle_{\pi^0} = 0.149 \pm 0.003$ GeV²/c² in π^+p interactions. These values are somewhat higher than those shown in Table VI but are not inconsistent with them.

VII. SUMMARY AND CONCLUSIONS

From the study of inclusive γ production in π^-p and π^+p interactions at 18.5 GeV/c, we have determined the inclusive γ cross sections as a function of charged prong number n and the inclusive π^0 production cross sections. We find that the average number of π^0 mesons, $\langle n_{\pi^0} \rangle = \frac{1}{2}\langle n_\gamma \rangle$, does not depend strongly on n at this energy.

The total inclusive π^0 cross section in π^-p interactions is consistent with the inclusive π^+ cross section and is significantly lower than the π^- cross section. In π^+p interactions the inclusive π^0 cross section is significantly lower than π^+ cross section, but is only slightly larger than the π^- cross section.

We have investigated the π^0 differential invariant cross section as a function of the Feynman variable x , and have compared these with the same distributions for π^- and π^+ production. Comparisons have been made in three different ways:

(1) We have computed γ spectra by a Monte Carlo method assuming that the π^0 momentum distribution corresponds to that of the π^- or π^+ mesons. These computed distributions have been compared with the experimentally observed γ spectra. From this comparison we conclude that the π^0 spectrum is more like that of the π^+ mesons in the π^-p interactions and like that of the π^- mesons in the π^+p interactions.

(2) We have used the Sternheimer approximation to derive the π^0 spectra from the experimentally observed γ spectra and have compared the derived π^0 spectra with observed π^- and π^+ spectra in the laboratory frame. This comparison also confirms

TABLE VI. Values of $\langle p_T \rangle$ and $\langle p_T^2 \rangle$ for inclusive γ and pions.

Inclusive particle	π^-p reaction		π^+p reaction	
	$\langle p_T \rangle$ (GeV)	$\langle p_T^2 \rangle$ (GeV ²)	$\langle p_T \rangle$ (GeV)	$\langle p_T^2 \rangle$ (GeV ²)
γ	0.172 ± 0.0002	0.052 ± 0.001	0.177 ± 0.002	0.053 ± 0.001
π^0	0.304 ± 0.030	0.125 ± 0.013	0.297 ± 0.030	0.122 ± 0.012
π^+	0.336 ± 0.003	0.185 ± 0.002	0.362 ± 0.002	0.201 ± 0.001
π^-	0.342 ± 0.001	0.170 ± 0.001	0.311 ± 0.001	0.140 ± 0.001

the conclusion that the π^0 spectrum is more like the π^+ spectrum in the π^-p case and like the π^- spectrum in the π^+p case.

(3) We have reconstructed the $\pi^0 \rightarrow 2\gamma$ events and have determined the x distribution of π^0 mesons after normalizing it to the measured total cross section. This method yields inclusive π^0 cross sections for small x directly and supports the conclusions reached via the above two indirect methods.

We have also studied the transverse momentum distributions of γ 's. These distributions are essentially the same whether one assumes the π^0 spectrum to be the same as the π^- spectrum or the π^+ spectrum.

We conclude that, in $\pi^\pm p$ interactions, inclusive π^0 cross sections and momentum spectra are consistent with those for secondary pions having opposite charge from the incident pion. They differ significantly from cross sections and momentum spectra for secondary pions of the same charge as the incident pion.

ACKNOWLEDGMENTS

We would like to thank the staffs of the 80-in. bubble chamber and the AGS at Brookhaven National Laboratory for their cooperation. The cooperation of W. L. Rickhoff, R. L. Erichsen, and the Notre Dame scanning and measuring staff is acknowledged with appreciation.

†Work supported in part by the National Science Foundation.

¹N. N. Biswas, N. M. Cason, V. P. Kenney, J. T. Powers, W. D. Shephard, and D. W. Thomas, *Phys. Rev. Lett.* **26**, 1589 (1971); J. T. Powers, Ph.D. thesis, University of Notre Dame, 1972 (unpublished); J. T. Powers, N. N. Biswas, N. M. Cason, V. P. Kenney, and W. D. Shephard, *Phys. Rev. D* **8**, 1947 (1973).

²V. P. Kenney *et al.*, in *Particles and Fields—1973*, proceedings of the Berkeley Meeting of the Division of Particles and Fields of the A.P.S., edited by H. H. Bingham, M. Davier, and G. R. Lynch (A.I.P., New York, 1973); P. T. Go *et al.*, Notre Dame Report No. 74-27 (unpublished).

³P. H. Stuntebeck, N. M. Cason, J. M. Bishop, N. N. Biswas, V. P. Kenney, and W. D. Shephard, *Phys. Rev. D* **9**, 608 (1974); P. H. Stuntebeck, Ph.D. thesis, University of Notre Dame, 1973 (unpublished).

⁴The results are not sensitive to this assumption. For example, if one assumes that 5% of the nonassociated γ events appear as associated in SQUAW fitting, then one gets a 2% contamination of such events in the final sample. However, no cases have been observed where a single γ links with two or more primary vertices (multiple events in a single frame).

⁵B. Rossi, *High Energy Particles* (Prentice-Hall, New York, 1952), p. 81.

⁶T. M. Knasel, DESY Reports Nos. 70/2 and 70/3, 1970 (unpublished).

⁷B. Rossi, *High Energy Particles* (Prentice-Hall, New York, 1952), p. 79.

⁸The topological cross sections for 18.5-GeV/c π^-p and π^+p interactions have been reported in Ref. 1. Note

that in calculating $\gamma(\pi^0)$ multiplicities we have used inelastic 2-prong and total inelastic cross sections.

⁹H. Bøggild *et al.*, *Nucl. Phys.* **B27**, 285 (1971); J. H. Campbell *et al.*, *Phys. Rev. D* **8**, 3824 (1973); G. Charlton *et al.*, *Phys. Rev. Lett.* **30**, 574 (1973); F. T. Dao *et al.*, *ibid.* **30**, 1151 (1973).

¹⁰J. W. Elbert *et al.*, *Nucl. Phys.* **B19**, 85 (1970); O. Balea *et al.*, Bucharest-Budapest-Cracow-Dubna-Hanoi-Serpukhov-Sofia-Tashkent-Tbilisi-Ulan Bator-Warsaw collaboration, *Nucl. Phys.* **B52**, 414 (1973); D. Bogert *et al.*, in *Particles and Fields—1973*, proceedings of the Berkeley Meeting of the Division of Particles and Fields of the A.P.S., edited by H. H. Bingham, M. Davier, and G. R. Lynch (A.I.P., New York, 1973).

¹¹M. E. Binkley *et al.*, *Phys. Lett.* **45B**, 294 (1973); A. R. Erwin, in *Proceedings of the XVI International Conference on High Energy Physics, Chicago-Batavia, Ill., 1972*, edited by J. D. Jackson and A. Roberts (NAL, Batavia, Ill., 1973), Vol. 1, p. 262.

¹²Rutherford-Ecole Polytechnique-Saclay collaboration, in *Proceedings of the Second International Conference on Elementary Particles, Aix-en-Provence, 1973* [*J. Phys. (Paris) Suppl.* **34**, C1-497 (1973)].

¹³R. M. Sternheimer, *Phys. Rev.* **99**, 277 (1955); R. G. Glasser, *Phys. Rev. D* **6**, 1933 (1972).

¹⁴R. N. Cahn, *Phys. Rev. Lett.* **29**, 1481 (1972); *Phys. Rev. D* **7**, 247 (1973).

¹⁵The values for π^- mesons have been previously published in Ref. 1. The values for π^+ mesons are preliminary (see Ref. 2).

¹⁶G. I. Kopylov, *Nucl. Phys.* **B52**, 126 (1973).